JA

The Iron K_α Line Profile in NGC 4151

T. Yaqoob, R. Edelson, K.A. Weaver, R.S. Warwick, R.F. Mushotzky, P.J. Serlemitsos, and S.S. Holt

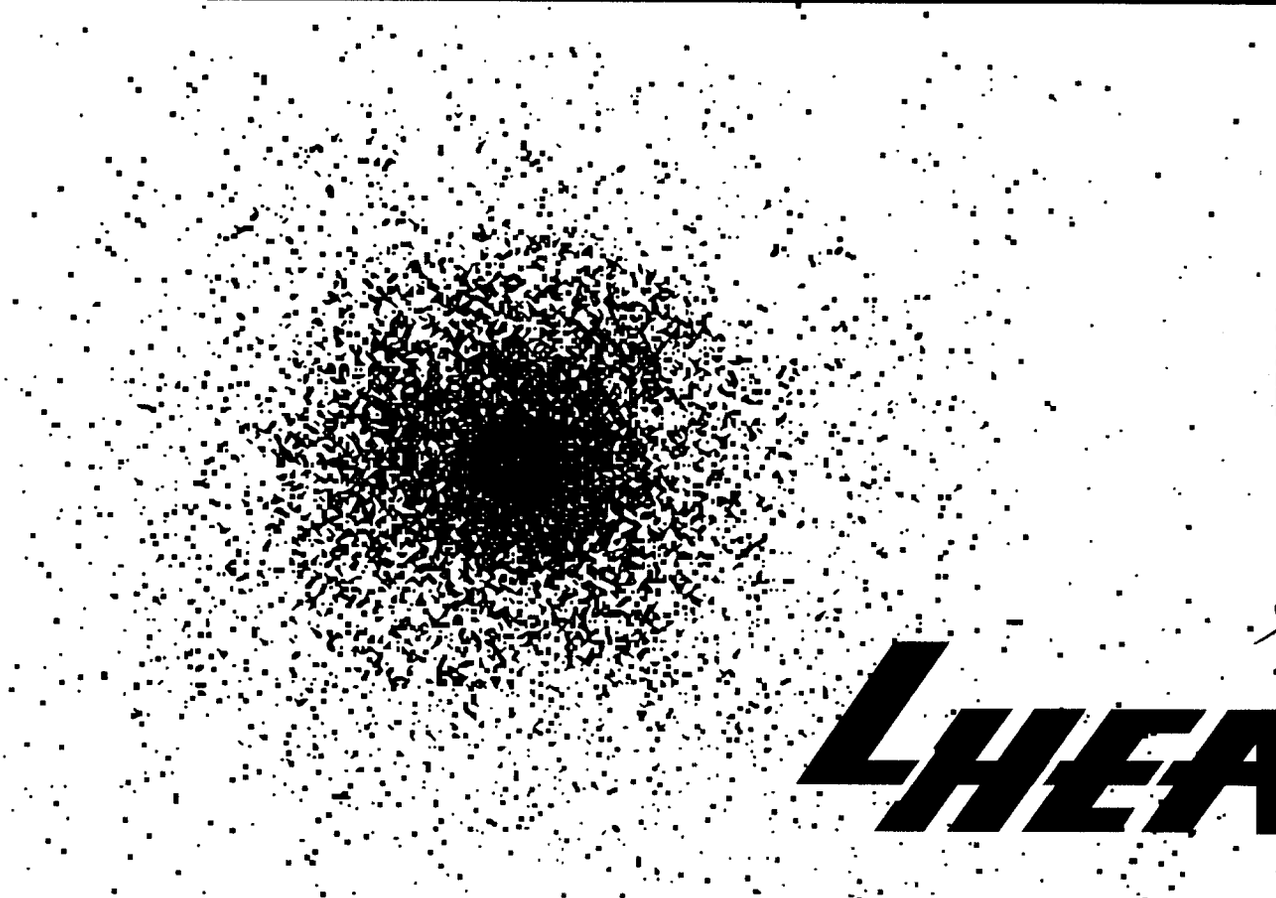

SW9544

LHEA

LABORATORY FOR HIGH ENERGY ASTROPHYSICS

National Aeronautics And Space Administration
Goddard Space Flight Center
Greenbelt, Maryland 20771

X-RAY: 95-20

THE IRON K_α LINE PROFILE IN NGC 4151

T. Yaqoob[1], R. Edelson[2], K.A. Weaver[3], R.S. Warwick[4],

R.F. Mushotzky, P.J. Serlemitsos, and S.S. Holt

Code 666
X-ray Astrophysics Branch
Laboratory for High Energy Astrophysics
NASA/Goddard Space Flight Center
Greenbelt, Maryland 20771

To appear in The Astrophysical Journal Letters, November 10, 1995

[1]Universities Space Research Association
[2]Now at University of Iowa
[3]Pennsylvania State University, now at Johns Hopkins University
[4]Dept. Physics and Astronomy, University of Leicester

ABSTRACT

We present the first measurements of the Fe K_α line profile in NGC 4151 from *ASCA* observations performed in May, November and December 1993. The apparent line profile is asymmetric, consisting of a peak at $\sim 6.3 - 6.4$ keV, a sharp drop on the blue side below ~ 7 keV and a broad red wing extending to $\sim 4 - 5$ keV. This first clear indication of complex structure confirms earlier tentative measurements of the Fe-K region with *BBXRT*. The line intensity, equivalent width and detailed shape are model-dependent. Interpretation of the profile in terms of emission from a disk rotating around a central black hole strongly constrains the putative disk to be face-on, but this contradicts the current body of knowledge of the geometry of this source. If the apparent red wing is not in fact part of a peculiar continuum then a face-on disk may be allowed only if the collimated structure observed at the parsec scale is misaligned with respect to the disk normal by at least 20 degrees, iron is overabundant by a factor of ~ 2, with some additional caveats. Alternatively, a different geometry of line-emitting material may be required. In contrast to clear variability in the soft X-ray line emission below ~ 1 keV between the observations, these data show no significant variability of the Fe K_α overall line shape, intensity or equivalent width.

Subject headings: black hole physics – galaxies: active – galaxies: individual: NGC 4151 – line: profiles – X-rays: galaxies

1. Introduction

It has long been recognized that measurement of the variability and shape of the Fe K_α fluorescence line found in many active galactic nuclei (AGN) at ~ 6.4 keV could provide an important tracer of matter in the heart of the nucleus, which is thought to harbour a super-massive black hole. Doppler and gravitational energy shifts of the line photons would imprint characteristic signatures on the line profile which map the geometric and dynamical distributions of matter around the black hole. Such effects may already have been observed by *ASCA* (see Tanaka, Inoue and Holt 1994, hereafter T94) in at least three Seyfert 1 galaxies, namely NGC 5548, IC 4329A (Mushotzky *et al.* 1995, hereafter M95) and MCG −6−30−15 (Tanaka *et al.* 1995, hereafter T95; Fabian *et al.* 1995, hereafter F95). The latter is the only case so far in which the statistics allow the line profile to be measured. Additional information concerning the geometry of matter in the active nucleus could in principle be derived from studying the *variability* of the line shape and intensity and its relationship to the continuum (e.g. Matt and Perola 1992). So far searches for such variability have been hindered by a lack of repeated observations with good statistics, sampling and energy resolution.

Many observations of the Seyfert 1.5 galaxy NGC 4151 ($z = 0.0033$) with low energy resolution proportional counter experiments indicated that if the Fe K_α line is narrow (FWHM $\sim 10^3$ km s^{-1} or less) then its intensity is consistent with a constant (average value $\sim 2.2 \times 10^{-4}$ photons cm^{-2} s^{-1}) as the underlying continuum varies by nearly an order of magnitude (Perola *et al.* 1986; Yaqoob *et al.* 1993, hereafter Y93). However, the data suggested that the line FWHM may be as high as $\sim 38,000$ km s^{-1} (Yaqoob & Warwick 1991). In the case that the line is truly broad it was not possible to determine whether the line intensity varied. Improved energy resolution observations with *BBXRT* hinted at a complex Fe K_α line shape consisting of a narrow core (FWHM $\sim 7,500$km s^{-1})

superimposed on a broader component (Weaver *et al.* 1992, hereafter W92). Still, limited statistics hampered attempts to constrain the apparently complex line profile.

In this paper we investigate the shape and variability of the Fe K_α line in NGC 4151 with better energy resolution and statistics than ever before, using three *ASCA* observations (see Table 1). Analyses of the very complex continuum in the 0.5–10 keV *ASCA* band have been reported in Weaver *et al.* (1994a, hereafter W94a) for Obs 1 and 2 and in Warwick *et al.* (1995a, hereafter W95a) for Obs 3. Details of the *ASCA* data and reduction can be found in W94a and W95a. See also Warwick, Done and Smith (1995b, hereafter W95b) for a discussion of *ROSAT / Ginga* spectra and Weaver *et al.* (1994b, hereafter W94b) for *BBXRT* observations. See T94 for a description of the *ASCA* instruments.

2. A Simple Empirical Model

In general, physical parameters deduced for the iron line are sensitive to the way the underlying continuum is modelled. Thus, it is essential to consider the continuum carefully in order to demonstrate that any conclusions about the line are not artificial. The problem with NGC 4151 is that complex absorption and emission features across the entire 0.5–10 keV *ASCA* band mean that it is not possible to uniquely determine the form of the intrinsic continuum (see W94a). Therefore, following W94a, we will derive results assuming a power law with photon index, Γ, having values in a range consistent with measurements by previous high-energy experiments. In practice, we use a fiducial value of $\Gamma = 1.6$ and repeat all spectral analysis with extreme values of $\Gamma = 1.3$ and 1.9 (e.g. see Y93; W95a). We note that using the *OSSE* data simultaneous with Obs 3 (see W95a) does not help to constrain Γ because a spectral break may occur in the 10–60 keV gap. An upper limit on Γ would be possible if we could be sure the spectrum did not flatten in the gap before rolling over again. Zdziarski, Johnson, & Magdziarz (1995) discuss the *ASCA/ OSSE* data further.

A minimum of three continuum components in addition to the power law are required to model the *ASCA* data (W94a,b and W95b). These are (i) an ionized (or 'warm') absorber, (ii) a few percent of the intrinsic power law which is scattered into our line-of-sight by an extended medium which is spatially resolved (e.g. Morse *et al.* 1995), and (iii) soft optically-thin emission with $kT \sim 0.5$ keV if it is thermal. The absorber is thought to have a column density, $N_H \sim 10^{22-23}$ cm^{-2}, and be lightly photoionized by the central continuum because the energy of the Fe-K edge is ~ 7.3 keV (Y93, W94a,b). Now, the presence of the Fe-K edge itself affects *in detail* the deduced shape of the Fe-K line. The Fe-K edge parameters depend on the ionization state of the absorber, which is in turn dependent upon *all* of the continuum components (i)–(iii). Figure 1 illustrates the rich soft and hard residual X-ray emission-line structure when the Obs 1–3 data are fitted with the above baseline model, excluding component (iii). One can clearly see by eye that the soft X-ray emission-line spectrum below ~ 1 keV varied and this is the first report of such variability in any AGN. Details and the refinement of models to account for the line-like features below 3 keV will be discussed in future work. In all three observations the Fe K_α line appears to consist of a narrow core and a broad red wing, very similar to MCG $-6-30-15$ (T95).

In order to focus on the Fe-K features we require an approach which avoids the complexities below 3 keV. Above 3 keV the power law and warm absorber dominate the continuum. Warm absorber parameters derived by ignoring data below 3 keV are not physically meaningful so we shall use a simple empirical model for the warm absorber opacity. We find that at an energy, E, between 3 and 10 keV, the power law plus warm absorber spectrum can be well modelled (apart from a normalization constant) by $N(E) = E^{-\Gamma} \exp[-(E/E_R)^{-\kappa}]\ K(E)$ photons cm^{-2} s^{-1} keV^{-1}, where $K(E) = \exp[-\tau^0_{\rm Fe}(E/E_K)^{-3}]$ above the Fe-K edge threshold energy (E_K) and unity otherwise ($\tau^0_{\rm Fe}$ is the optical depth at threshold). This works well for any part of warm absorber parameter space unless the data can discriminate between a complex Fe-K edge

and the simple Fe-K edge model above. Caution should be exercised in interpreting the parameter $\tau_{\rm Fe}^0$ since we are not using a physical model for the soft X-ray opacity. The parameters E_R and κ model the soft X-ray cutoff but have no physical meaning. It is important to note that we will quantify the effect of varying Γ on the deduced iron line parameters and this effect is much larger than that of substituting the analytic model for the warm absorber. A further advantage of our approach is that we can directly investigate the Fe-K edge energy and optical depth. Note that we do not include a Compton-reflection continuum (e.g. George and Fabian 1991) in the fits because high energy experiments have not found evidence for one (Maisack and Yaqoob 1991; Y93). We searched extensively for other possible physical continuum forms which could mimic the red wing of the line. F95 independently did the same for MCG $-6-30-15$ so we do not repeat details here. Our conclusion is similar: the best-fitting solution is to modify the warm-absorber model by the addition of a cold absorber closer to the power-law source, with a covering fraction of $\sim 65\%$ and a column of $\sim 3.2 \times 10^{23}$ cm^{-2}. However, the steep photon index of $\Gamma \sim 2.3$ required to produce an acceptable fit is problematic.

Table 1 shows the results of fitting Obs 1–3 with the empirical model, plus two Gaussians (narrow and broad) for the Fe K_α line. All spectral fitting in this paper uses data from all four *ASCA* instruments (T94) and all parameters are rest-frame quantities. The three free parameters of the narrow line are E_N (center energy in keV), σ_N (intrinsic Gaussian width in keV) and I_N (intensity in units 10^{-4} photons cm^{-2} s^{-1}). Similarly, the broad line parameters are E_B, σ_B and I_B. Values of the difference in χ^2 ($\equiv \Delta\chi^2_{B-N}$; Table 1) between double- and single-Gaussian fits show that the requirement for the broad Gaussian is highly significant in all three observations. Even the smallest $\Delta\chi^2_{B-N}$ corresponds to a probability of 6.5×10^{-5} that the improved χ^2 for the double-Gaussian fit compared to a single-Gaussian fit is obtained by chance. Figure 2 illustrates the quality of fit and the line profile for for Obs 3.

From Table 1, the *observed* 4–10 keV instrument-averaged continuum flux, F_{4-10}(obs), varied by a factor $\sim$ 1.6 between Obs 1–3. Note that absolute *ASCA* fluxes and line intensities are subject to systematic uncertainty of the order of 10% (e.g. Yaqoob *et al.* 1994). The intrinsic flux is model dependent and since we do not know whether Γ varied, we cannot determine whether the intrinsic flux varied. However, making the most generous assumptions, that Γ varied from 1.3 to 1.6 between Obs 1 and Obs 3 and assuming the lowest model flux in Obs 1 (see footnote in Table 1) it is unlikely that the intrinsic 4–10 keV flux varied by more than a factor of 2. As for the iron line, there is a hint that the peak of the narrow component was higher in Obs 1 than in Obs 2 and 3 (see §3). However, there is no compelling evidence, within the errors, that the gross line shape, total intensity or equivalent width (EW) varied between Obs 1–3. This conclusion is independent of the assumed Γ. We find that the dependence of the narrow Gaussian parameters on Γ can be completely neglected compared to statistical errors and the sensitivity of the broad Gaussian to Γ is moderate (see Table 1). The measured intensities and EW of the narrow component in Obs 1–3 are all consistent with pre-*ASCA* measurements of the narrow line (e.g. Y93; W92). The broad component increases the total line intensity and EW by a factor $\sim$ 3 compared to the narrow line alone. We repeated the entire analysis in this section for the four 'snap-shots' comprising Obs 3 (see W95a) and again found no convincing evidence for variability in the line parameters.

3. Relativistic Disk Model And Physical Implications

If the line broadening were due to Compton scattering, the Fe-K edge would be smeared out (see also arguments in M95, T95 and F95). These arguments suggest that while Compton scattering may play *some* role in forming the line profile, it is unlikely to be the sole cause. Doppler and Gravitational broadening may then be important. Here we

test the data against a model in which line photons are emitted in a disk rotating around a central black hole (e.g. Fabian *et al.* 1989). This is the currently accepted 'canonical' model for broad Fe K_α lines in AGN and therefore our results can be easily and directly compared with others in the literature. We fit the highest statistical quality data (Obs 3) with the model in §2, replacing the double Gaussian by a disk plus Schwarzschild black hole model of the Fe K_α line (see Fabian *et al.* 1989). The parameters are $\theta_{\rm obs}$ (inclination angle of the disk normal relative to the observer), r_i (inner radius), r_o (outer radius), q (power-law index characterizing the line emissivity as $\propto r^{-q}$), $I_{\rm D}$ (intensity), and E_D (line energy in the disk rest frame). Preliminary spectral fitting showed that r_i is always forced to its minimum value of $6r_g$ ($r_g \equiv GM/c^2$) and the fits were insensitive to r_o. Therefore r_i and r_o are fixed at $6r_g$ and $10^3 r_g$ respectively. The results are shown in Table 2 for $\Gamma = 1.6$ (similar results are obtained for $\Gamma = 1.3$ and 1.9). The model is then fitted to Obs 1 and 2 with $\theta_{\rm obs}$ and q fixed at the best-fitting values for Obs 3 (see Table 2). Again there is no clear evidence for variability of the line shape, intensity or EW. Note the model dependence of the latter two quantities; the disk model gives values less than the sums of the double-Gaussian values in §2. The line center energies for Obs 2 and 3 are only just consistent with 6.4 keV but not so for Obs 1 (however, note the possible systematic uncertainty of $\sim 30 - 40$ eV in the energy scale). The apparent variability of the line energy requires investigation with better statistics. Note that $E_D > E_N$ is due to gravitational redshifting of the line peak. The inclination angle of the disk is strongly constrained to be face-on by Obs 3 ($\theta_{\rm obs} = 0^{+19}_{-0}$ degrees). This is because larger inclinations give a double-peaked line profile with a prominent blue Doppler horn but the observed line shows a sharp cutoff on the blue side. The result is robust with respect to choice of continuum. When we model the 0.5–10 keV data using a physical model with a warm absorber and continuum components in §2 we obtain a 90% confidence (6 parameter) upper limit on $\theta_{\rm obs}$ of 21 degrees.

The measured values of the Fe K_α EW are only marginally compatible with a cold,

solar abundance face-on disk which predicts an EW of $\sim 160 - 190$ eV ($\Gamma = 1.9$–1.3; George & Fabian 1991). However, the predicted Compton-reflection continuum from a disk with $\theta_{\rm obs} < 20$ degrees (e.g. see George & Fabian 1991; Matt, Perola and Piro 1991) exceeds the upper limits set by higher energy observations of NGC 4151 by a factor ~ 2 or more (Maisack & Yaqoob 1991; Y93). On the other hand, an over-abundance of iron by a factor of ~ 2 would be more compatible with the observed EW and a diminished reflection continuum. Still, some interpretations of the orientation of the biconical, collimated ionizing cones, the radio jet and the extended soft X-ray emission suggest an edge-on disk geometry (see Morse *et al.* 1995; Evans *et al.* 1993). The smallest inclination (~ 40 degrees) interpretation (Boksenberg *et al.* 1995 and references therein) may face problems with the observed NLR kinematics and the energy budget (Schulz 1995). Even without such problems, the collimated structures would have to be misaligned by at least ~ 20 degrees with respect to the disk normal to reproduce the observed iron line profile. It is also possible that the geometry at the parsec-scale does not reflect the geometry at the much smaller scale of the putative disk. Note that if the narrow core of the line had a separate origin (such as the BLR or a torus) and the residual broad component came from a disk, direct fitting shows that the inclination is still required to be face-on. If the unified scheme of Seyfert galaxies is correct, a contribution to the iron line from the putative torus is *expected* (Krolik, Madau, & Życki 1994). The disk model is only acceptable with the above caveats. We will explore other geometries, such as the blob model of Nandra & George (1994) in future work.

The authors wish to thank the *ASCA* operations personnel in Japan whose relentless efforts have made these and all other *ASCA* observations possible. The authors thank the International AGN Watch for the opportunity to work on the Obs 3 data and Brad Peterson, Andy Fabian, Paul Nandra, Lev Titarchuk, Sandip Chakrabarti, Andzrej Zdziarski and the referee, Dr. Ian Evans, for helpful suggestions.

REFERENCES

Boksenberg, A., *et al.* 1995, ApJ, 440, 151

Evans, I. N., Tsvetanov, Z., Kriss, G. A., Ford, H. C., Caganoff, S., & Koratkar, A. P. 1993, ApJ, 417, 82

Fabian, A. C., Nandra, K., Reynolds, C. S., Brandt, W. N., Otani, C., Tanaka, Y., Inoue, H., & Iwasawa, K. 1995, MNRAS, in press (F95)

Fabian, A. C., Rees, M. J., Stella, L., & White, N. E. 1989, MNRAS, 238, 729

George I. M., & Fabian A. C. 1991, MNRAS, 249, 352

Krolik, J. H., Madau, P., & Życki, P. T. 1994, ApJ, 420, L57

Maisack, M., & Yaqoob, T. 1991, A&A, 249, 25

Matt G., Perola G. C., & Piro L. 1991, A&A, 247, 25

Matt G., & Perola G. C., 1992, A&A, MNRAS, 259, 433

Morse, J. A., Wilson, A. S., Elvis, M., Weaver, K. A. 1995, ApJ, 439, 121

Mushotzky, R. F., Fabian, A. C., Iwasawa, K., Kunieda, H., Matsuoka, M., Nandra, K., & Tanaka, Y. 1995, MNRAS, 272, L9 (M95)

Nandra, K., & George, I. M. 1994, MNRAS, 267, 974

Perola, G. C., *et al.* 1986, APJ, 306, 508

Pounds K. A., Nandra K., Stewart G. C., George I. M., & Fabian A. C. 1990, Nat, 344, 132

Schulz, H. 1995, PhD Thesis, University of Ruhr, Bochum

Tanaka, Y., Inoue, H., & Holt, S. S. 1994, PASJ, 46, L137 (T94)

Tanaka, Y., *et al.* 1995, Nat, in press (T95)

Warwick, R. S., Done, C., & Smith, D. A. 1995b, MNRAS, in press (W95b)

Warwick, R. S., *et al.* 1995a, APJ, submitted (W95a)

Weaver K. A., *et al.* 1992, ApJ, 401, L11 (W92)

Weaver, K. A., *et al.* 1994, ApJ, 423, 621 (W94b)

Weaver, K. A., Yaqoob, T., Holt, S. S., Mushotzky, R. F., Matsuoka, M., Yamauchi, M. 1994, ApJ, 436, L27 (W94a)

Yaqoob, T., *et al.* 1994, PASJ, 46, L49

Yaqoob, T., & Warwick, R. S. 1991, MNRAS, 248, 773

Yaqoob T., Warwick R. S., Makino F., Otani C., Sokoloski J. L., Yamauchi Y., & Bond I. A. 1993, MNRAS, 262, 435 (Y93)

Zdziarski, A. A., Johnson, N. W., & Magdziarz, P. 1995, MNRAS, submitted.

This manuscript was prepared with the AAS LaTeX macros v3.0.

TABLE 1: Spectral Fits With An Empirical Model

	Obs 1	Obs 2	Obs 3
Date/ 1993	May 24–25	Nov 5	Dec 4–9
Exposure [a]	15.5	19.5	41.2
χ^2	1213	1171	1678
	(1212, 1213)	(1171, 1176)	(1674, 1684)
d.o.f. [b]	1258	1132	1548
E_R (keV)	$4.60^{+1.30}_{-0.52}$	$2.49^{+0.32}_{-0.43}$	$2.94^{+0.10}_{-0.09}$
	(3.68, 6.17)	(1.70, 3.73)	(2.49, 4.04)
κ	$1.63^{+0.27}_{-0.25}$	1.0 (f)	$1.97^{+0.41}_{-0.39}$
	(2.04, 1.34)	(2.53, 1.05)	(2.94, 1.38)
E_K (keV)	$7.11^{+0.09}_{-0.0}$	$7.26^{+0.41}_{-0.15}$	$7.20^{+0.19}_{-0.09}$
$\tau^0_{\rm Fe}$	$0.26^{+0.06}_{-0.05}$	$0.08^{+0.06}_{-0.05}$	$0.12^{+0.03}_{-0.03}$
E_B (keV)	$5.9^{+0.3}_{-0.5}$	$5.6^{+0.4}_{-0.4}$	$5.7^{+0.2}_{-0.3}$
	(5.9, 5.9)	(5.6, 5.8)	(5.6, 5.7)
σ_B (keV)	$0.9^{+0.5}_{-0.5}$	$0.9^{+0.8}_{-0.5}$	$0.7^{+0.3}_{-0.3}$
	(0.9, 0.9)	(0.9, 0.8)	(0.7, 0.7)
I_B [c]	$6.0^{+4.9}_{-2.8}$	$8.4^{+11.2}_{-5.0}$	$7.5^{+3.9}_{-3.6}$
	(5.1, 3.9)	(9.5, 7.3)	(8.3, 7.0)
EW_B (eV)	307^{+245}_{-145}	300^{+399}_{-178}	222^{+115}_{-107}
	(334, 247)	(337, 261)	(248, 206)
E_N (keV)	$6.41^{+0.08}_{-0.09}$	$6.35^{+0.06}_{-0.06}$	$6.35^{+0.05}_{-0.04}$
σ_N (keV)	$0.07^{+0.18}_{-0.07}$	$0.05^{+0.09}_{-0.05}$	$0.09^{+0.11}_{-0.08}$
I_N [c]	$2.2^{+3.2}_{-1.3}$	$2.5^{+1.5}_{-1.2}$	$2.7^{+1.7}_{-1.0}$
EW_N (eV)	126^{+185}_{-74}	102^{+60}_{-49}	92^{+57}_{-32}
F_{4-10}(obs) [d]	11.2	15.0	17.9
F_{4-10}(int) [e]	21.8	21.2	22.0
	(15.7, 30.1)	(14.8, 25.4)	(18.9, 30.4)
$\Delta\chi^2_{B-N}$	26	33	101
	(22, 34)	(42, 38)	(236, 89)

Notes for Table 1

The model parameters were derived using $\Gamma = 1.6$ but best-fitting values are also given for $\Gamma = 1.3$ and 1.9 (first and second values in parentheses respectively) for parameters which are sensitive to Γ. Note that the Γ which gives the minimum χ^2 is *not* necessarily the correct solution because we are ignoring the complexities in the data below 3 keV. We are only using Γ as a parameterization of the continuum in the Fe-K region. The number of free parameters, including four normalizations each, in the fits for Obs 1, 2 and 3 are 14, 13 and 14 respectively (κ had to be frozen, indicated by (f), in Obs 2 to avoid the fit becoming unstable in the error analysis). In order to further avoid the spectral fits becoming unstable, the Fe-K edge parameters had to be frozen at their best-fit values in order to derive the errors for all model components except the narrow Gaussian. Likewise, the errors on the Fe-K edge parameters had to be derived by freezing all the remaining model parameters (except normalizations). Additionally for Obs 1, the broad Gaussian parameters were frozen to derive errors on κ and E_R and κ were frozen to derive errors on the broad Gaussian parameters. The quoted errors are 90% confidence and the number of interesting parameters in each case is equal to the number of free parameters minus the number of frozen parameters minus the number of normalizations (four). For reference, the critical changes in χ^2 from the minima, for 2, 5, 6, 7, 8, 9 and 10 parameters of interest, are 4.61, 9.24, 10.65, 12.01, 13.36, 14.68 and 15.99 respectively. Note that the lower errors on the Fe-K edge energy (E_K) are not statistical since E_K is not allowed be less than 7.11 keV.

[a] Mean exposure time (Ks) for 4 instruments.

[b] d.o.f. = degrees of freedom.

[c] Intensity of broad and narrow iron line components in units of 10^{-4} photons cm^{-2} s^{-1}.

[d] Observed 4–10 keV flux in units of 10^{-11} erg cm^{-2} s^{-1}.

[e] Intrinsic 4–10 keV flux in the above units. Note that this does *not* include the line fluxes. Note also that for Obs 1 and 2, the intrinsic flux is $\sim$ 70% lower if a physical model of a warm absorber is used instead of the empirical opacity model.

TABLE 2: Relativistic Disk Model Spectral Fits

	Obs 1	Obs 2	Obs 3
χ^2	1230	1193	1689
d.o.f. [a]	1261	1137	1550
E_D (keV)	$6.60^{+0.07}_{-0.09}$	$6.48^{+0.05}_{-0.06}$	$6.50^{+0.06}_{-0.08}$
I_D [b]	$5.8^{+1.8}_{-1.7}$	$6.1^{+1.9}_{-1.9}$	$7.2^{+1.6}_{-2.0}$
EW_D (eV)	307^{+93}_{-90}	245^{+75}_{-75}	241^{+53}_{-67}
q	2.63 (f)	2.63 (f)	$2.63^{+0.19}_{-0.28}$
$\theta_{\rm obs}$ (deg)	0.0 (f)	0.0 (f)	$0.0^{+19.0}_{-0.0}$
r_i/r_g	6.0 (f) (< 9.0)	6.0 (f) (< 7.8)	6.0 (f) (< 7.8)

Errors correspond to 90% confidence for 6, 5 and 8 interesting parameters for Obs 1, Obs 2 and Obs 3 respectively (see notes for Table 1). Fixed parameters are indicated by (f). The model for Obs 1 has two less free parameters than Obs 3 because q and $\theta_{\rm obs}$ are fixed at their best-fitting values for Obs 3. These are also fixed in Obs 2 which also has κ fixed (see Table 1). The upper limits for r_i/r_g correspond to 90% confidence for 7, 6 and 9 interesting parameters for Obs 1, Obs 2 and Obs 3 respectively.

[a] d.o.f. = degrees of freedom.

[b] Disk iron line intensity in units of 10^{-4} photons cm^{-2} s^{-1}.

Figure Captions

Figure 1

The result of fitting Obs 1–3 data with the baseline warm absorber model discussed in §2 (and used by W94a) but omitting the soft optically-thin continuum emission and the Fe K_α line. This clearly illustrates the rich line-emission structures across the *ASCA* bandpass. Below 3 keV emission due to O, Fe L (and possibly Ne), Si and S is evident. Shown are the ratios of the data from the two Solid-State Imaging Spectrometers (SIS) to the best-fitting model. The data are binned at approximately the energy resolution of the detectors, which is $\Delta E/E \sim 2\%$ at 5.9 keV.

Figure 2

(a) Ratio of Obs 3 data from the two Solid-state Spectrometers (SIS) to the best-fitting double-Gaussian model described in §2. (b) as (a) but for the data from the two GIS Imaging Spectrometers (GIS) which have poorer energy resolution than the SIS ($\Delta E/E \sim 8\%$ at 5.9 keV). (c) As (a) but with the intensities of the broad and narrow Fe K_α line components set to zero. (d) As (c) for the GIS data.

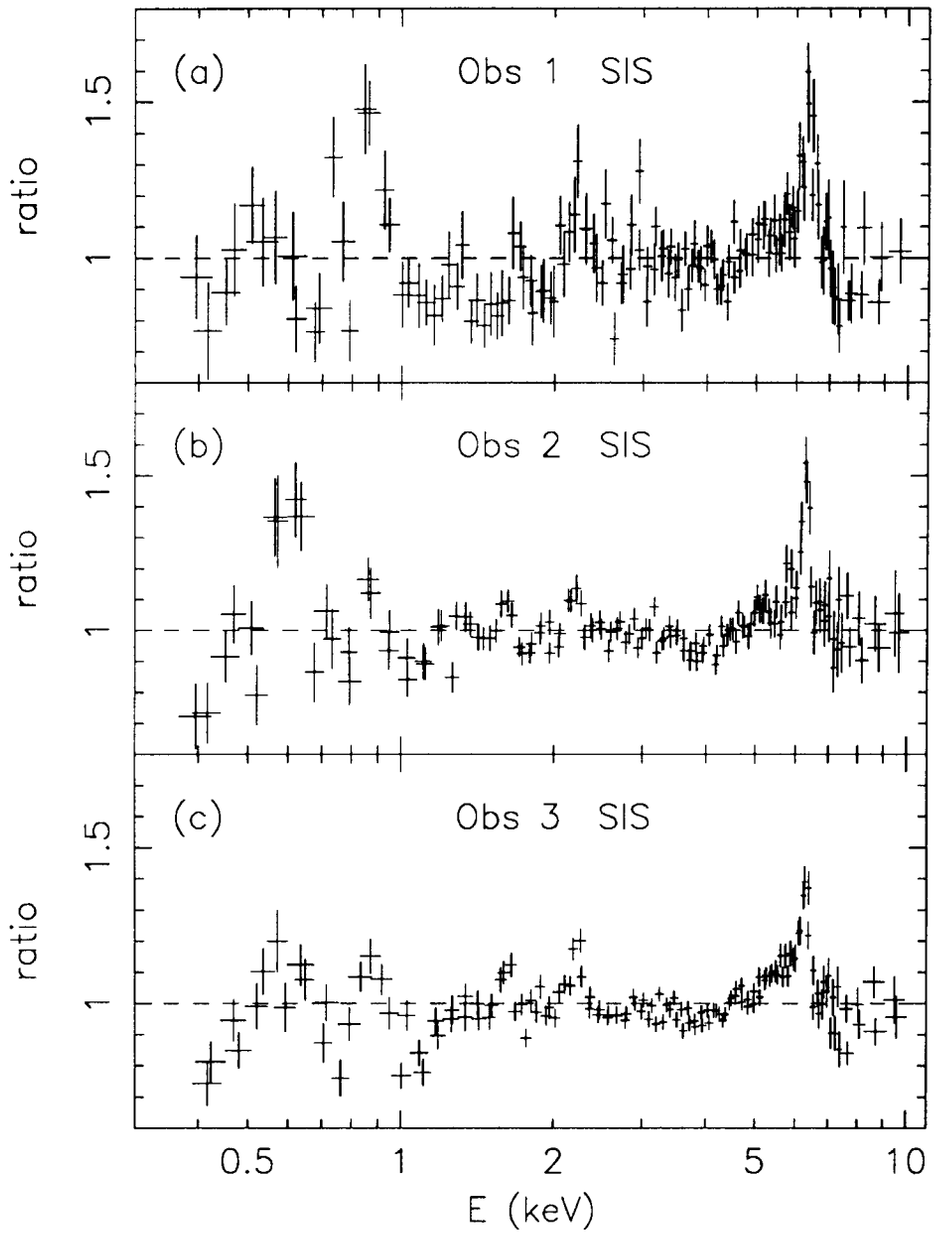

Figure 1

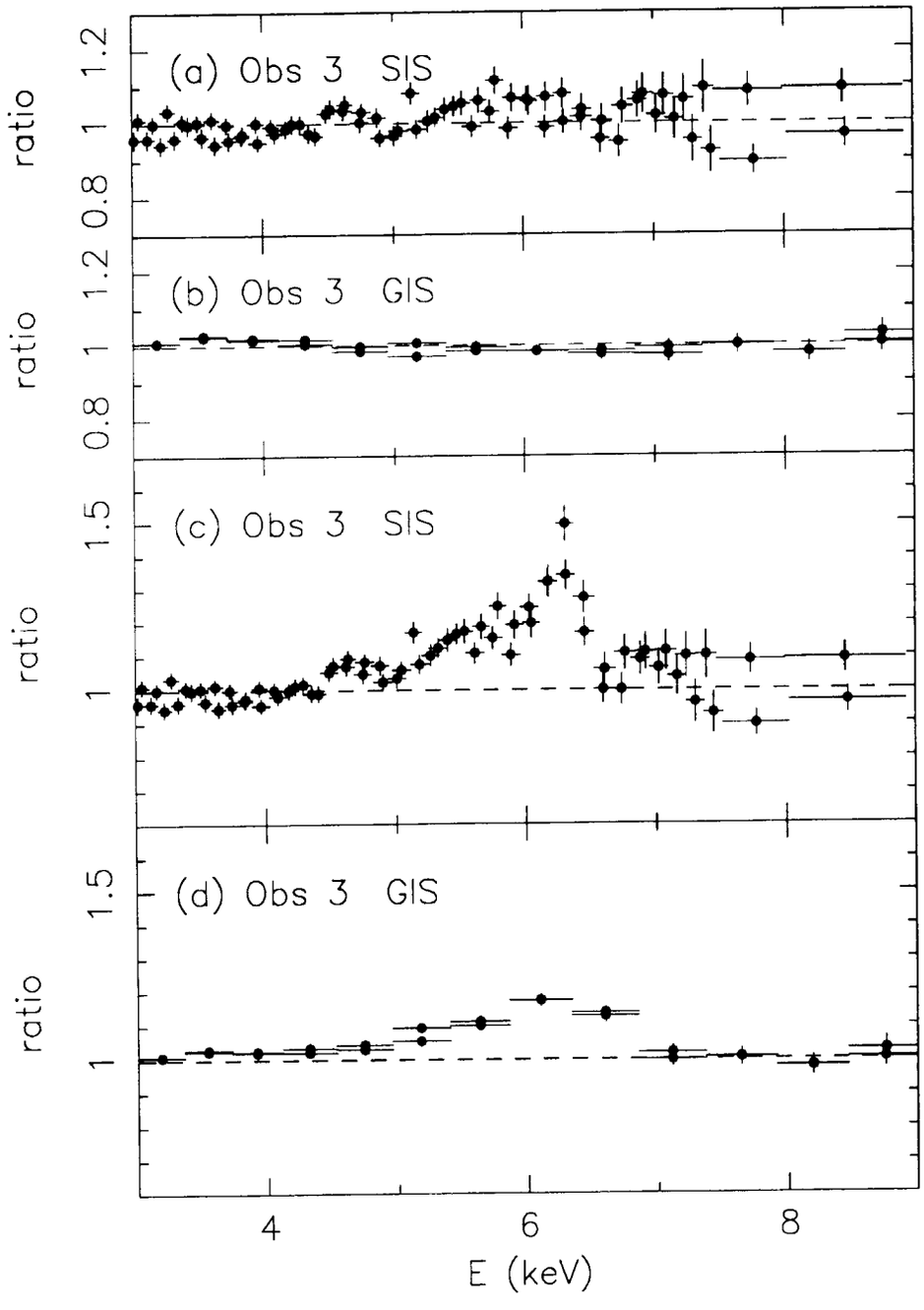

Figure 2